PHYSICAL REVIEW A **76**, 011802(R) (2007)

Quasi-phase-matching of high-order harmonics using a modulated atomic density

T. Auguste, B. Carré, and P. Salières
Service des Photons, Atomes et Molécules, CEA-Saclay, 91191 Gif-sur-Yvette Cédex, France
(Received 21 July 2006; published 9 July 2007)

We present a numerical study of high-order harmonic generation in a gas medium with spatial modulation of the density. We show that, by adjusting the modulation period, the contributions of the short and long quantum paths to harmonic emission can be selectively quasi-phase-matched on axis. In particular, quasi-phase-matching of the short path contribution dramatically improves the spatial and spectral properties of the harmonic beam, increasing peak brightness by a factor close to 40 for the 45th harmonic of a Ti:sapphire laser at 17.8 nm. Finally, simultaneous or selective quasi-phase-matching of the short and long paths makes it possible to control their relative weight.

DOI: 10.1103/PhysRevA.76.011802 PACS number(s): 42.65.Ky, 32.80.Rm

With the advances in the technology of short-pulse high-power lasers, many experimental and theoretical works have investigated the generation of high-order harmonics (HOHs) of intense laser pulses interacting with gases [1]. Considerable progress has been made in characterizing and optimizing HOHs over a broad spectral range. This ultrashort coherent extreme ultraviolet (xuv) source is now used in a growing number of applications, such as time-resolved and nonlinear studies in diluted, condensed, and plasma phases [2]. However, many applications, e.g., nonlinear studies, remain difficult on account of the small number of photons generated per pulse. Several trails have been investigated to increase this number, aiming at controlling the key condition of phase matching. The relevant parameters are the absorption length $L_{abs}=1/\sigma\rho$ (σ is the ionization cross section, and ρ the atomic density) and the coherence length L_{coh}, defined as the distance over which the nonlinear polarization and the harmonic field get dephased by π, i.e., over which the harmonic field builds constructively; it is expressed as $\pi/\Delta k$, where Δk is the wave vector (phase gradient) mismatch between the two fields. Beyond L_{coh}, phase mismatch leads periodically to destructive interferences. An optimal conversion efficiency in a long uniform medium is obtained when $L_{coh}>5L_{abs}$ [3]. To be meaningful, the increase of L_{coh}, which is a local quantity, far above L_{abs} should be achieved at each point throughout the medium, over a distance of the order of L_{abs} itself. As a rule, this requires that the laser wave front and the medium be optimized in a uniform or slowly varying geometry, such as in a gas-filled hollow-core fiber [3,4], gas cell [5], or long gas jet [6]. Such absorption-limited emission has been demonstrated for intermediate harmonic orders, but is difficult to reach for high orders, for which L_{abs} is large (in the millimeter range). A second trail for improving the conversion efficiency thus consists in *quasi-phase-matching* (QPM), that is, either "reversing" or canceling the nonlinear process in the medium region where the polarization and the harmonic field are initially out of phase. In "perturbative" nonlinear optics, QPM is routinely used to correct the phase mismatch, e.g., by reversing periodically the orientation of the nonlinear crystal at intervals L_{coh} [7]. For HOHs in the vacuum ultraviolet, while a phase-corrective scheme has been theoretically proposed [8], QPM proposals rather aim at canceling the out-of-phase emission. This can be done in two ways: (i) by modulating the atomic density along the laser axis [9], and (ii) by modulating the generating laser beam. In the case of a laser beam guided in a hollow-core fiber, a periodic modulation of the fiber inner diameter results in a modulation of the peak intensity. If the modulation period is twice the coherent length of the cutoff harmonics, a clear enhancement of these harmonics is observed, shifting the spectrum up to the water window in neon [10]. An aperiodic groove spacing (linearly chirped fiber) has been proposed in order to quasi-phase-match a large number of harmonic orders with different coherence lengths [11]. In the case of a laser beam focused in a gas cell or jet, a relatively weak counterpropagating beam can disrupt the generation in regions with destructive contribution to the emission, so that a quasi-phase-matched regime is achieved [12].

In this paper, we study theoretically QPM of high-order harmonics by spatial modulation of the atomic density. The main advance is that, in contrast to previous work in the perturbative regime [9], we take full account of the nonperturbative atomic dipole, and in particular of its intensity-dependent phase, which plays a crucial role in phase matching [13]. We show that the contributions of, respectively, the short and long quantum paths [14] to HOH emission can be selectively quasi-phase-matched on axis. They can also be simultaneously optimized, on and off axis, whereas they remain clearly distinguishable in their spectral and spatial properties. We finally show that one can optimize the density modulation and QPM, so that the brightness of the 45th harmonic of a Ti:sapphire laser increases by a factor close to 40.

The numerical model we use has been described in [15]. Briefly, the two-dimensional code in cylindrical geometry solves the coupled propagation equations of the fundamental and harmonic fields in the paraxial and slowly varying envelope approximations. The source term in the propagation equation of the harmonic field, i.e., the induced nonlinear polarization, is calculated nonperturbatively within the strong-field approximation [16]. The optical field ionization of the gas is described by the Ammosov-Delone-Kraïnov tunneling model [17]. The resulting depletion of the medium and free-electron dispersion are included in the propagation equations, as well as the atomic dispersion and the absorption of the harmonic field. We consider a Ti:sapphire laser pulse, spatially Gaussian with a confocal parameter $b=5$ mm, temporally Gaussian with a 50 fs full width at half maximum (FWHM), focused at $I_0=6\times10^{14}$ W/cm^2 peak in-

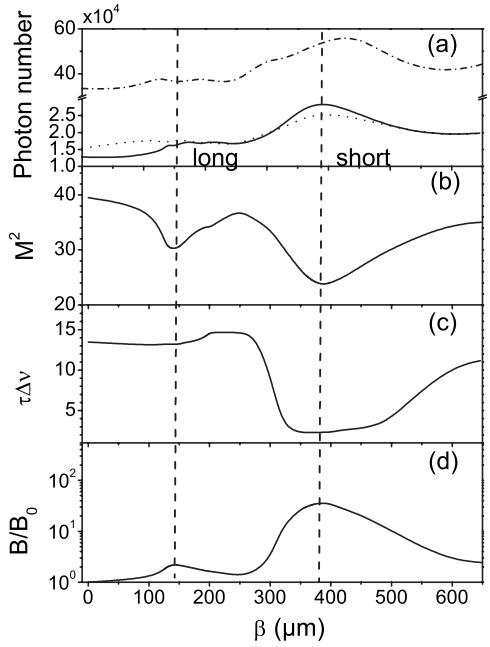

FIG. 1. (a) Number of photons in H45 generated in neon as a function of the modulation period β for $\alpha=1$, $P_0=10$ Torr, $I_0=6\times10^{14}$ W/cm^2; (b) evolution of the M^2 factor; (c) $\tau\times\Delta\nu$ product; (d) brightness normalized to $\alpha=0$ case. In (a), the solid (dotted) line corresponds to the case without (with) ionization, and the dot-dashed line to $P_0=60$ Torr with ionization. The dashed lines emphasize quasi-phase-matching for the long and the short quantum paths, respectively.

tensity, 1 mm after a 10 Torr neon gas jet ($z_0=+1$ mm). In these conditions, phase matching is mainly controlled by the geometric Gouy phase and the dipole phase, and not by the atomic and electronic dispersions [13,18]. These are thus good conditions to test QPM by density modulation, since this technique cannot compensate for index-related phase mismatches [9]. The envelope of the jet density profile is a truncated Lorentzian (at 20% of the peak density) with FWHM $2z_L=800$ μm along the direction of laser propagation z, and is uniform in the transverse direction. The normalized modulated density along the z axis is given by $n_0(z)=\{1-(\alpha/2)[1-\cos(2\pi z/\beta)]\}/[1+(z/z_L)^2]$, where α and β are the amplitude and the period of the modulation, respectively. For the sake of comparison, the computations are carried out for a constant number of atoms in the jet. This means that the peak pressure (set to 10 Torr in the absence of modulation) is increased up to 20 Torr, depending on α and β, when the modulation is on. In a first step, the medium ionization is not taken into account.

In Fig. 1(a), we report the number of photons emitted in the 45th harmonic (H45) as a function of the modulation period β for $\alpha=1$, i.e., for a maximum modulation amplitude. The number of photons first increases with β, reaches a plateau at 160 μm, then increases to a maximum at 390 μm, and finally decreases. The maximum photon number is 2.2 times larger than that obtained with a Lorentzian profile ($\alpha=0$).

To get deeper insight in the computed behavior, we calculate the different contributions to the phase mismatch. In the strong-field regime, the phase-matching condition is written [18] $\vec{k}_q=q\vec{k}_1+\vec{\nabla}\varphi_q=q\vec{k}_1-\alpha_q\vec{\nabla}I$, where q is the harmonic order, $\vec{k}_1$ the laser wave vector, $\vec{k}_q$ the harmonic wave vector, and φ_q the phase of the atomic dipole. The origin of this intrinsic phase is the action acquired by the electron wave packet along the trajectory leading to the emission of the qth harmonic. It can be approximated by $\varphi_q\simeq-U_p\tau_t\simeq-\alpha_q I$, where U_p is the ponderomotive potential and τ_t the electron travel time. In a first approximation, φ_q varies linearly with the laser intensity I; the slope α depends on the travel time, and exhibits a weak dependence on both the laser intensity and the harmonic order except close to the cutoff region. In fact, it has a quite generic behavior for the high harmonics. When the harmonic is in the deep-plateau region, there are mainly two trajectories leading to the emission, corresponding, respectively, to $\alpha_q^{short}\simeq1\times10^{-14}$ rad cm^2/W and $\alpha_q^{long}\simeq24\times10^{-14}$ rad cm^2/W [19–21]. In the cutoff region, these two trajectories merge into a single trajectory, characterized by $\alpha_q^{cutoff}\simeq13.7\times10^{-14}$ rad cm^2/W. Focusing the laser in the nonlinear medium may thus result in large longitudinal and transverse gradients of the φ_q phase that have a major influence on phase matching. Due to the different slopes, the best phase-matching conditions are different for the different trajectories. The contribution of the dipole phase to the phase mismatch on axis can be written

$$\nabla\varphi_q=-\alpha_q\nabla I=\frac{8(z-z_0)b^2}{[b^2+4(z-z_0)^2]^2}\alpha_q I_0. \quad (1)$$

In our conditions, at the center of the jet, $\nabla\varphi_q^{short}\simeq-14$ cm^{-1} for the short trajectory, while $\nabla\varphi_q^{long}\simeq-336$ cm^{-1} for the long one. The other important term introduced by focusing is the geometric dispersion due to the phase advance on axis, i.e., the Gouy phase. Because of the multiplying factor q, the Gouy phase affects first the nonlinear polarization, so that the geometric wave vector mismatch reduces to $\Delta k_{geo}\simeq q\Delta k_{1,geo}=-2qb/[b^2+4(z-z_0)^2]=-155$ cm^{-1}. This gives a total mismatch on axis of $\Delta k=\nabla\varphi_q+\Delta k_{geo}=-169$ cm^{-1} for the short trajectory and -491 cm^{-1} for the long one. The corresponding coherence lengths $L_{coh}=\pi/|\Delta k|$ are equal, respectively, to 190 and 60 μm. They are shorter than the medium length, so that efficient harmonic emission is hindered on axis in both cases. However, the large transverse gradient of the long quantum path allows it to be phase matched off axis, as shown in [18]. If we now modulate the atomic density with a period equal to twice the coherence length, the out-of-phase emission will be canceled, allowing an efficient construction of the harmonic field on axis. Indeed, our above estimates of the optimal periods (380 and 120 μm) are very close to the ones derived from complete simulations (390 and 160 μm).

In order to strengthen this interpretation, we plot in Fig. 2 the radially integrated H45 intensity as a function of the position along the propagation axis in the generating medium. In the absence of density modulation (dotted line), the signal grows very slowly due to the destructive interferences occurring on axis. By contrast, with a density profile modulated at a period $\beta=390$ μm (solid curve), the signal increases rapidly, by steps of approximately 400 μm. A very

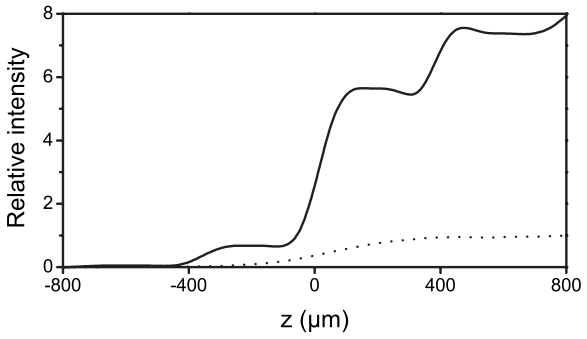

FIG. 2. H45 intensity increase along propagation for $\alpha=0$ (dotted curve), and for $\alpha=1$ and $\beta=390$ μm (solid curve).

similar behavior is obtained for the H45 intensity on axis. This demonstrates that the short trajectory is quasi-phase-matched on axis.

This is even clearer in Figs. 3(a) and 3(b) giving, respectively, the H45 near- and far-field profiles calculated with modulated (solid curves) and unmodulated (dotted lines) density profiles. In the latter case, as previously mentioned, the chosen focusing conditions favor selectively the long path that is phase matched off axis. This results in an annular emission with a minimum on axis in the near- and far-field profiles. When the modulation is turned on, the short path contribution builds up on axis, giving a maximum in the spatial profiles, especially pronounced in the far field. Simultaneoulsy, the off-axis phase matching for the long path does not seem affected by the modulation. Due to the slower intensity dependence of φ_q^{short}, the short path contribution has a smaller phase front curvature, and thus a smaller divergence. This results in a significant improvement of the beam quality [22], as clearly shown in Fig. 1(b) displaying the evolution of the quality factor M^2. For a beam with cylindrical symmetry, it is defined as $M^2=\sqrt{(\langle r^2\rangle\langle\theta^2\rangle-\langle r\theta\rangle^2)}$, where r is the normalized radial and θ the divergence coordinate in the beam. M^2 is currently used as an estimate of the deviation from a pure Gaussian beam ($M^2=1$), which seems very large

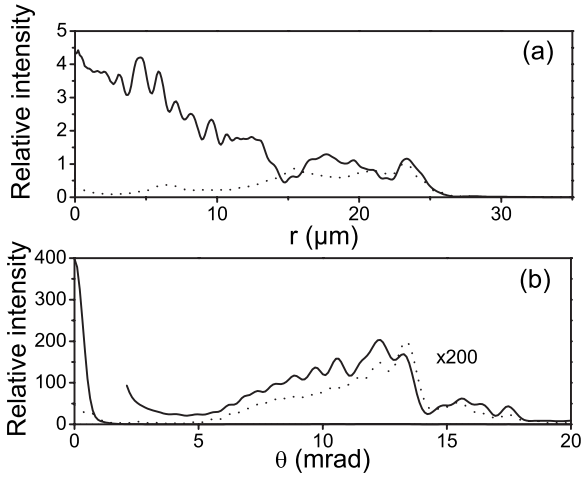

FIG. 3. (a) Near-field profiles of H45 calculated for $\alpha=0$ (dotted curve), and for $\alpha=1$ and $\beta=390$ μm (solid curve). (b) Corresponding far-field profiles.

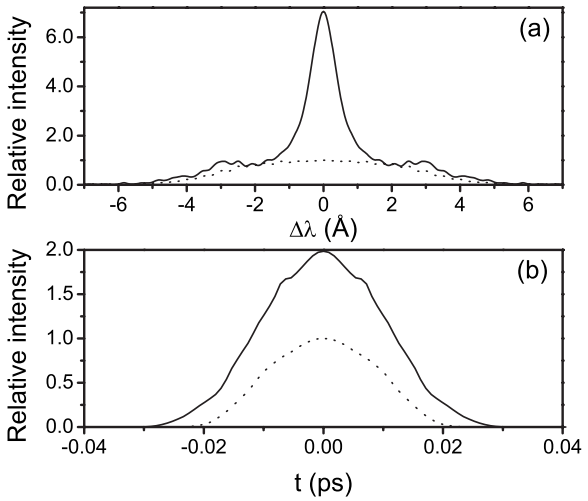

FIG. 4. (a) Power spectra of H45 calculated for $\alpha=0$ (dotted curve), and for $\alpha=1$ and $\beta=390$ μm (solid curve). (b) Corresponding temporal profiles.

in Fig. 1(b). However, note that the broad off-axis distribution retains a dominant weight in the calculated value. The M^2 factor restricted to the close-to-axis highly collimated beam, i.e., the short path contribution, is very close to 1, i.e., the beam is Gaussian. The beam quality is also somewhat improved around $\beta=150$ μm, where the long trajectory is quasi-phase-matched on axis.

The onset of the short trajectory contribution for $\beta=390$ μm is clearly evidenced in the spectrum in Fig. 4(a), as a high narrow central peak ($\Delta\lambda\approx 1$ Å) on top of the broad wings that correspond to the long trajectory (dotted curve). Indeed, the slower intensity dependence of the short trajectory results in a smaller frequency chirp of the emission, and thus a narrower spectrum [20,23]. The temporal envelope shown in Fig. 4(b) is not affected by the density modulation: the pulse duration τ is equal to 24 fs (FWHM) in both cases. Note that the harmonic emission is confined to the top of the laser envelope where the laser intensity does not vary much, so that the values of the slopes α_q^{short} and α_q^{long} are roughly constant during the interaction [19,21]. The product $\tau\times\Delta\nu$ is thus considerably reduced, as shown in Fig. 1(c). It drops from 12 for $\beta=100$ μm to 2 for $\beta=390$ μm. This directly impacts on the source peak brightness, defined as the number of photons per 0.1% bandwidth per mm^2 per mrad^2 per s, which increases by a factor of 36 compared to the case without modulation. In addition to the number of photons generated, it reflects the overall spatial, spectral, and temporal properties of the source. Brightness is actually the most relevant criterion of performance for many applications, such as time-resolved interferometry, which exploits the temporal and spatial coherence of the source.

Then we carried out simulations including the medium ionization. The main change is a 10% decrease of the number of photons [see Fig. 1(a)] but the optimum value of β is not modified, confirming that, in our conditions, phase matching is governed by geometric factors rather than electron dispersion. When the pressure is increased to 60 Torr, ionization effects become more pronounced, with a 30% signal decrease, while the atomic dispersion results in a slightly

larger optimum β value, but the QPM effect is still clearly there. The conversion efficiency reaches 2×10^{-8}, only a factor of 2–3 smaller than that obtained at the absorption limit by Schnürer *et al.* and Hergott *et al.* [5,6]. However, an absorption-limited emission is usually associated with important beam distortions due to large atomic and electronic dispersions [22], and thus to a reduced brightness. In our conditions, QPM allows us to get good beam quality and high brightness while preserving the attosecond structure that is very sensitive to the electronic dispersion. Finally, computations performed for different values of the modulation amplitude α (for constant β) show a monotonic evolution of the QPM process; namely, we observe a continuous narrowing of the harmonic spectrum, and the near- and far-field profiles get more and more peaked on axis as the value of α is increased from 0 to 1.

In summary, we have shown that a periodic modulation of the atomic density allows one to quasi-phase-match *on axis* the contributions of either the short or the long quantum path. The modulation period, adjusted to twice the coherence length associated with either path, serves as a control parameter. It allows one to dramatically enhance the contribution of the short trajectory to the on-axis emission, through improved beam quality and spectral sharpness. This results in a gain by a factor of 36 in peak brightness at 17.8 nm. The phase-matched off-axis emission from the long trajectory is not affected by the modulation, so that the short and long quantum path contributions can be simultaneously optimized. However, they remain clearly identified, and thus can be discriminated, in their spectral and spatial properties.

Experimentally, the density modulation could be obtained either from an acoustic wave (in the supersonic range around 100 kHz), or by using a nozzle with periodically spaced holes [24]. This opens very interesting perspectives for optimizing the brightness of the harmonic source, the relevant criterion for a number of applications. In addition, quasi-phase-matching offers a way to control the relative weight of the two quantum paths. This control is highly relevant for generating attosecond pulses from phase-locked, synchronized spectral components [25,26]; it also conditions phase-dependent applications of the ultrashort xuv pulses. Finally, our QPM technique could be useful for enhancing the contributions of the longer quantum paths, which have so far never been observed due to their large phase mismatch.

This research was partially supported by the Marie Curie Research Training Network XTRA (Grant No. MRTN-CT-2003-505138) and the Integrated Initiative of Infrastructure LASERLAB-EUROPE (Grant No. RII3-CT-2003-506350, FOSCIL).

[1] P. Salières *et al.*, Adv. At., Mol., Opt. Phys. **41**, 83 (1999).
[2] A. L'Huillier *et al.*, Eur. Phys. J. D **26**, 91 (2003).
[3] E. Constant *et al.*, Phys. Rev. Lett. **82**, 1668 (1999).
[4] A. Rundquist *et al.*, Science **280**, 1412 (1998); R. Bartels *et al.*, Nature (London) **406**, 164 (2000).
[5] M. Schnürer *et al.*, Phys. Rev. Lett. **83**, 722 (1999); Y. Tamaki, J. Itatani, Y. Nagata, M. Obara, and K. Midorikawa, *ibid.* **82**, 1422 (1999); S. Kazamias *et al.*, *ibid.* **90**, 193901 (2003).
[6] J.-F. Hergott *et al.*, Phys. Rev. A **66**, 021801(R) (2002); V. Tosa, E. Takahashi, Y. Nabekawa, and K. Midorikawa, *ibid.* **67**, 063817 (2003).
[7] J. A. Armstrong, N. Bloembergen, J. Ducuing, and P. S. Pershan, Phys. Rev. **127**, 1918 (1962).
[8] I. P. Christov, H. C. Kapteyn, and M. M. Murnane, Opt. Express **3**, 360 (1998); I. P. Christov, Phys. Rev. A **60**, 3244 (1999).
[9] P. L. Shkolnikov, A. Lago, and A. E. Kaplan, Phys. Rev. A **50**, R4461 (1994).
[10] I. P. Christov, H. C. Kapteyn, and M. M. Murnane, Opt. Express **7**, 362 (2000); E. A. Gibson *et al.*, Science **302**, 95 (2003); A. Paul *et al.*, Nature (London) **421**, 51 (2003).
[11] I. P. Christov, J. Opt. Soc. Am. B **18**, 1877 (2001).
[12] S. L. Voronov *et al.*, Phys. Rev. Lett. **87**, 133902 (2001).
[13] P. Salières, A. L'Huillier, and M. Lewenstein, Phys. Rev. Lett. **74**, 3776 (1995).
[14] M. Lewenstein, P. Salières, and A. L'Huillier, Phys. Rev. A **52**, 4747 (1995).
[15] A. L'Huillier, P. Balcou, S. Candel, K. J. Schafer, and K. C. Kulander, Phys. Rev. A **46**, 2778 (1992).
[16] M. Lewenstein, P. Balcou, M. Y. Ivanov, A. L'Huillier, and P. B. Corkum, Phys. Rev. A **49**, 2117 (1994).
[17] M. V. Ammosov, N. B. Delone, and V. P. Kraïnov, Sov. Phys. JETP **64**, 1191 (1986).
[18] Ph. Balcou, P. Salières, A. L'Huillier, and M. Lewenstein, Phys. Rev. A **55**, 3204 (1997).
[19] Ph. Balcou, A. Dederichs, M. B. Gaarde, and A. L'Huillier, J. Phys. B **32**, 2973 (1999).
[20] P. Salières *et al.*, Science **292**, 902 (2001).
[21] M. B. Gaarde and K. J. Schafer, Phys. Rev. A **65**, 031406(R) (2002).
[22] L. Le Déroff, P. Salières, and B. Carré, Opt. Lett. **23**, 1544 (1998).
[23] M. B. Gaarde *et al.*, Phys. Rev. A **59**, 1367 (1999).
[24] B. N. Chichkov *et al.*, Phys. Rev. A **52**, 1629 (1995).
[25] Y. Mairesse *et al.*, Science **302**, 1540 (2003).
[26] H. Merdji *et al.*, Phys. Rev. A **74**, 043804 (2006).